

Tutorial on Power Swing Blocking and Out-of-Step Tripping

Normann Fischer, Gabriel Benmouyal, Daqing Hou,
Demetrios Tziouvaras, John Byrne-Finley, and Brian Smyth
Schweitzer Engineering Laboratories, Inc.

Presented at the
39th Annual Western Protective Relay Conference
Spokane, Washington
October 16–18, 2012

Tutorial on Power Swing Blocking and Out-of-Step Tripping

Normann Fischer, Gabriel Benmouyal, Daqing Hou, Demetrios Tziouvaras, John Byrne-Finley, and Brian Smyth,
Schweitzer Engineering Laboratories, Inc.

Abstract—Power systems are operated with such tight stability margins that when a power system experiences a fault or disturbance, the generator rotors are subject to severe oscillations. These oscillations in the generator rotor angle translate into severe power flow oscillations (or power swings) across the system. The occurrence of a power swing condition on a power system must be detected, and the appropriate protective action needs to be taken.

For a stable power swing, it is possible that the positive-sequence impedance trajectory will traverse the operating region of a distance element. In this case, the distance element needs to be blocked from operating using power swing blocking (PSB); otherwise, an unwanted operation of a distance element can occur, further weakening an already weakened system. Therefore, it is important that all power swing conditions be detected as rapidly as possible to prevent any unwanted operation of the protection system.

For unstable power swings (or out-of-step conditions), out-of-step tripping (OST) is implemented to separate the network into islands with a generation-load balance. Stability studies determine the locations where it is best to detect the out-of-step conditions and separate the system into islands. All other locations need to implement PSB so as not to separate the system at unwanted locations. OST comes with its own challenges, such as when a trip command should be issued or if the system can regain stability after experiencing a pole slip.

This paper is a tutorial on how distance relays cope with power swing conditions on the power system. It discusses different methods of detecting power swings and the best method to separate the system to maintain stability and avoid a major blackout if a power swing condition becomes unstable.

I. INTRODUCTION

A balance between generated and consumed active power exists during steady-state operating conditions and is necessary for the stability of the power system. Power system disturbances cause oscillations in machine rotor angles that can result in severe power flow swings. Depending on the severity of the disturbance and the actions of power system controls, the system may remain stable or experience a large separation of generator rotor angles and eventually lose synchronism. Large power swings can cause unwanted relay operations that can further aggravate the power system disturbance and cause major power outages or blackouts.

A power swing blocking (PSB) function is available in modern distance relays to prevent unwanted distance relay element operation during power swings. The out-of-step tripping (OST) function discriminates between stable and unstable power swings and initiates network islanding during loss of synchronism between power system areas.

Traditional PSB and OST functions may use dual-quadrilateral characteristics that are based on the measurement of the time it takes the positive-sequence impedance to cross the two blinders. An extensive number of power system stability studies may be required, taking into consideration different operating conditions, in order to determine the settings for the dual-quadrilateral PSB and OST functions. This is a costly exercise, and we can never be certain that all possible scenarios and operating conditions were considered.

The swing center voltage (SCV) method calculates the positive-sequence SCV rate of change and does not require any stability studies or user settings for the proper blocking of relay elements. This method is well suited for long, heavily loaded transmission lines that pose significant problems for traditional power swing detection methods.

After reviewing some of the different methods used for PSB and OST, this paper presents a performance comparison between the traditional dual-quadrilateral method and the SCV variation method for both PSB and OST. The performances of both methods are analyzed using field data obtained from a system disturbance and transient simulation data obtained from a Real Time Digital Simulator (RTDS[®]).

II. POWER SWINGS AND OUT-OF-STEP PHENOMENON

A power swing is a system phenomenon that is observed when the phase angle of one power source starts to vary in time with respect to another source on the same network. The phenomenon generally occurs following a major disturbance, like a fault, that alters the mechanical equilibrium of one or more machines. A power swing is stable when, following a disturbance, the rotation speed of all machines returns to synchronous speed. A power swing is unstable when, following a disturbance, one or more machines do not return to synchronous speed, thereby losing synchronism with the rest of the system.

A. Basic Phenomenon Using the Two-Source Model

The simplest network for studying the power swing phenomenon is the two-source model, as shown in Fig. 1. The left source has a phase angle advance equal to θ , and this angle will vary during a power swing. The right source represents an infinite bus, and its angle will not vary with time. As simple as it is, this elementary network can be used to model the phenomena of more complex networks.

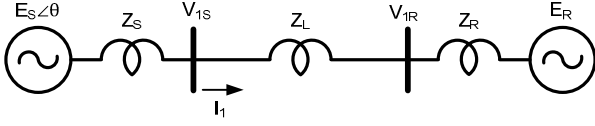


Fig. 1. Two-source equivalent elementary network.

B. Representation of Power Swings in the Impedance Plane

Assuming the sources have equal impedance amplitude, for a particular phase angle θ , the location of the positive-sequence impedance (Z_1) calculated at the left bus is provided by the following equation [1]:

$$Z_1 = \frac{V_{1S}}{I_1} = Z_T \cdot \frac{E_S \angle \theta}{E_S \angle \theta - E_R} - Z_S \quad (1)$$

In (1), Z_T is the total impedance, as in:

$$Z_T = Z_S + Z_L + Z_R \quad (2)$$

Assuming the two sources are of equal magnitude, the Z_1 impedance locus in the complex plane is given by (3).

$$Z_1 = \frac{Z_T}{2} \cdot \left(1 - j \cot \frac{\theta}{2} \right) - Z_S \quad (3)$$

When the angle θ varies, the locus of the Z_1 impedance is a straight line that intersects the segment Z_T orthogonally at its middle point, as shown in Fig. 2. The intersection occurs when the angular difference between the two sources is 180 degrees. When a generator torque angle reaches 180 degrees, the machine is said to have slipped a pole, reached an out-of-step (OOS) condition, or lost synchronism.

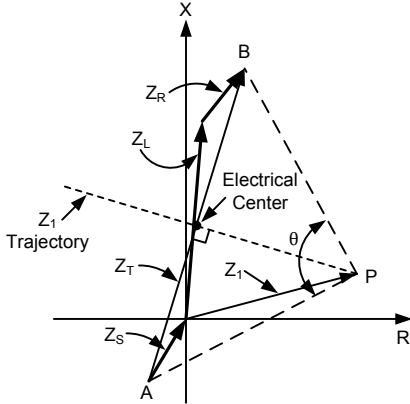


Fig. 2. Locus of the Z_1 impedance during a power swing with sources of equal magnitude.

When the two sources have unequal magnitudes such that n is the ratio of E_S over E_R , the locus of the Z_1 impedance trajectory will correspond to the circles shown in Fig. 3. For any angle θ , the ratio of the two segments joining the location of the extremity of Z_1 (Point P) to the total impedance extremities A and B is equal to the ratio of the source magnitudes.

$$n = \frac{E_S}{E_R} = \frac{PA}{PB} \quad (4)$$

The precise equation for the center and radius of the circles as a function of the ratio n can be found in [1].

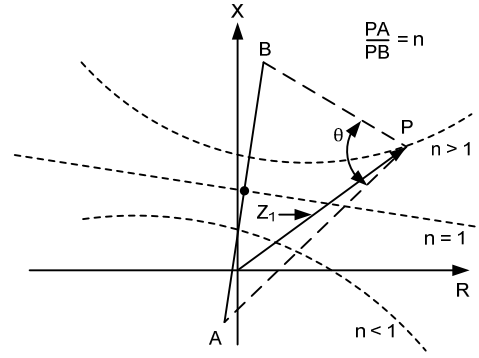


Fig. 3. Locus of the Z_1 impedance during a power swing with sources of unequal magnitude.

It should be noted that, in reality, a power source is a synchronous generator and is therefore not an ideal voltage source as represented in the equivalent two-source model. Furthermore, the impact of any existing automatic voltage regulator must be considered. During a power swing, the ratio of two power source magnitudes is not going to remain constant. Therefore, the resulting locus of the Z_1 impedance will switch from one circle to another, depending upon the instantaneous magnitude ratio [2].

C. Rate of Change of the Positive-Sequence Impedance

Starting with (1) and assuming the two sources are of equal magnitude, the time derivative of the Z_1 impedance is provided by (5).

$$\frac{dZ_1}{dt} = -jZ_T \cdot \frac{e^{-j\theta}}{(1 - e^{-j\theta})^2} \cdot \frac{d\theta}{dt} \quad (5)$$

Assuming the phase angle has a linear variation with a slip frequency in radians per second given as:

$$\frac{d\theta}{dt} = \omega \quad (6)$$

and using the identity:

$$|1 - e^{-j\theta}| = 2 \cdot \sin \frac{\theta}{2} \quad (7)$$

the rate of change of the Z_1 impedance is finally expressed as:

$$\left| \frac{dZ_1}{dt} \right| = \frac{|Z_T|}{4 \cdot \sin^2 \frac{\theta}{2}} \cdot |\omega| \quad (8)$$

Equation (8) expresses the principle that the rate of change of the Z_1 impedance depends upon the sources, transmission line impedances, and the slip frequency, which, in turn, depends upon the severity of the perturbation.

As a consequence, any algorithm that uses the Z_1 impedance displacement speed in the complex plane to detect a power swing will depend upon the network impedances and the nature of the perturbation. Furthermore, contrary to the positive-sequence line impedance, the source impedances are not introduced into the relay so the relay cannot usually predict the displacement speed.

Fig. 4 shows the normalized plot of the rate of change of the Z_1 impedance as a function of the phase angle θ . The minimum value is 1, corresponding to θ equals 180 degrees. In order to obtain the real value of the rate of change, the vertical axis has to be multiplied by:

$$\frac{|Z_T|}{4} \cdot |\omega| \quad (9)$$

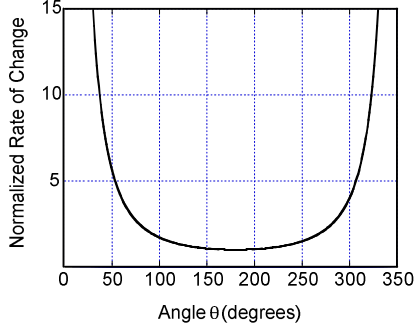


Fig. 4. Normalized rate of change of the Z_1 impedance.

Fig. 4 also shows that the higher the total impedance (Z_T) and slip frequency, the higher the minimum value of the Z_1 impedance rate of change. Note that the region of importance for PSB and OST is the flat segment of the curve in Fig. 4.

D. The Justification for Detecting Power Swings

There are two reasons why power swings should be detected. First, they can lead to the misoperation of directional comparison schemes, generation protection, or some protection elements, such as Zone 1 distance, phase overcurrent, or phase undervoltage. For these instances, a PSB signal is needed to ensure the security of the elements. Second, in the case of an unstable swing, a network separation is needed in order to avoid a network collapse. In this instance, the OOS condition must be detected in order to generate an OST signal.

III. POWER SWING DETECTION METHODS

There are many different methods that are used to detect power swings, each with its strengths and drawbacks. This section presents some of those detection methods.

A. Conventional Rate of Change of Impedance Methods

The rate of change of impedance methods are based on the principle that the Z_1 impedance travels in the complex plane with a relatively slow pace (see Fig. 4), whereas during a fault, Z_1 switches from the load point to the fault location almost instantaneously.

1) Blinder Schemes

Fig. 5 shows an example of a single-blinder scheme. This scheme detects an unstable power swing when the time interval required to cross the distance between the right and left blinders exceeds a minimum time setting. The scheme allows for the implementation of OST on the way out of the zone and cannot be used for PSB because the mho characteristics will be crossed before the power swing is detected. This method is most commonly implemented in conjunction with generator protection and not line protection.

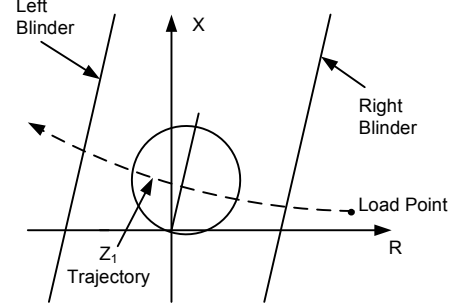


Fig. 5. Single-blinder characteristic.

Fig. 6 shows an example of a dual-blinder scheme. During a power swing, the single-blinder element measures the time interval ΔT that it takes the Z_1 trajectory to cross the distance between the outer and inner blinders. When this measured time interval is longer than a set time delay, a power swing is declared. The set time delay is adjusted so that it will be greater than the time interval measured during a fault and smaller than the time interval measured during the Z_1 travel at maximum speed. Using the dual-blinder scheme, an OST scheme can be set up to either trip on the way into the zone or on the way out of the zone.

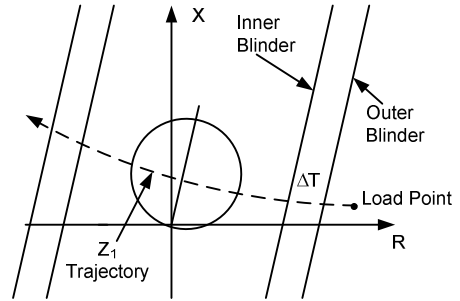


Fig. 6. Dual-blinder characteristic.

2) Concentric Characteristic Schemes

Concentric characteristics for the detection of power swings work on the same principle as dual-blinder schemes: after an outer characteristic has been crossed by the Z_1 impedance, a timer is started and the interval of time before the inner characteristic is reached is measured. A power swing is detected when the time interval is longer than a set time delay. Characteristics with various shapes have been used, as shown in Fig. 7. The dual-quadrilateral characteristic represented at the bottom right of Fig. 7 has been one of the most popular.

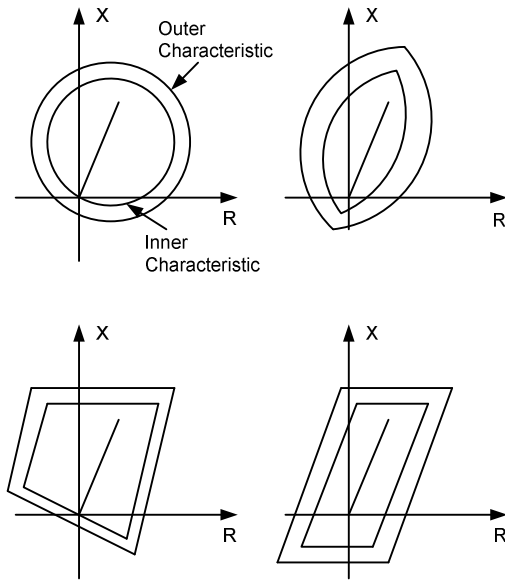


Fig. 7. Concentric characteristics of various shapes.

B. Issues Associated With the Concentric or Dual-Blinder Methods

1) Impact of the System Impedances on the PSB Function

To guarantee enough time to carry out blocking of the distance elements after a power swing is detected, the inner impedance of the blinder element must be placed outside the largest distance element for which blocking is required. In addition, the outer blinder impedance element should ideally be placed away from the load region to prevent PSB logic operation caused by heavy loads, thus establishing an incorrect blocking of the line mho tripping elements.

The previous requirements are difficult to achieve in some applications, depending on the relative line impedance and source impedance magnitudes [3]. Fig. 8 shows a simplified representation of one line interconnecting two generating sources in the complex plane with a swing locus bisecting the total impedance. Fig. 8a depicts a system in which the line impedance is large compared with system impedances (strong source), and Fig. 8b depicts a system in which the line impedance is much smaller than the system impedances (weak source).

We can observe from Fig. 8a that the swing locus could enter the Zone 2 and Zone 1 relay characteristics during a stable power swing from which the system could recover. For this particular system, it may be difficult to set the inner and

outer PSB blinder elements, especially if the line is heavily loaded, because the necessary PSB settings are so large that the load impedance could establish incorrect blocking. To avoid incorrect blocking resulting from load, lenticular distance relay characteristics, load encroachment, or blinders that restrict the tripping area of the mho elements have been applied in the past. On the other hand, the system shown in Fig. 8b becomes unstable before the swing locus enters the Zone 2 and Zone 1 mho elements, and it is relatively easy to set the inner and outer PSB blinder elements.

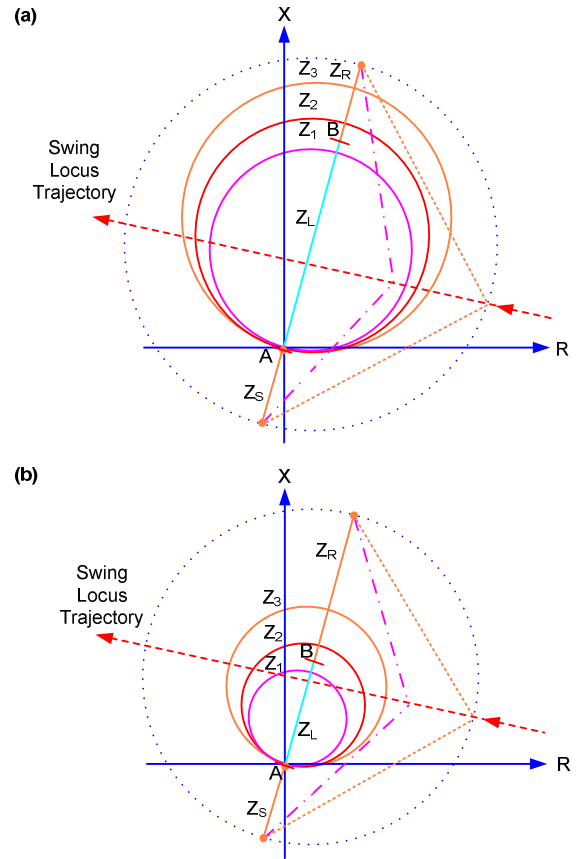


Fig. 8. Effects of source and line impedances on the PSB function.

Another difficulty with the blinder characteristic method is the separation between the inner and outer PSB blinder elements and the timer setting that is used to differentiate a fault from a power swing. These settings are not difficult to calculate, but depending on the system under consideration, it may be necessary to run extensive stability studies to determine the fastest power swing and the proper PSB blinder element settings. The rate of slip between two systems is a function of the accelerating torque and system inertias. In general, a relay cannot determine the slip analytically because of the complexity of the power system. However, by performing system stability studies and analyzing the angular excursions of systems as a function of time, we can estimate an average slip in degrees per second or cycles per second. This approach may be appropriate for systems where slip frequency does not change considerably as the systems go out of step. However, in many systems where the slip frequency

increases considerably after the first slip cycle and on subsequent slip cycles, a fixed impedance separation between the blinder PSB elements and a fixed time delay may not be suitable to provide a continuous blocking signal to the mho distance elements.

In a complex power system, it is very difficult to obtain the proper source impedances that are necessary to establish the blinder and PSB delay timer settings [4]. The source impedances vary continuously according to network changes, such as additions of new generation and other system elements. The source impedances could also change drastically during a major disturbance and at a time when the PSB and OST functions are called upon to take the proper actions. Note that the design of the PSB and OST functions would have been trivial if the source impedances remained constant and if it were easy to obtain them. Normally, very detailed system stability studies are recommended in order to consider all contingency conditions in determining the most suitable equivalent source impedance to set the PSB or OST functions.

2) Impact of Heavy Load on the Resistive Settings of the Quadrilateral Element

References [4] and [5] recommend setting the concentric dual-quadrilateral power swing characteristic inside the maximum load condition but outside the maximum distance element reach desired to be blocked. In long-line applications with a heavy load flow, following these settings guidelines may be difficult, if not impossible. Fortunately, most numerical distance relays allow some form of programming capability to address these special cases. However, in order to set the relay correctly, stability studies are required; a simple impedance-based solution is not possible.

The approach for this application is to set the power swing blinder such that it is inside the maximum load flow impedance and the worst-case power swing impedance, as shown in Fig. 9. Using this approach can result in cutting off part of the distance element characteristic. Reference [6] provides additional information and logic to address the issues of PSB settings in heavily loaded transmission lines.

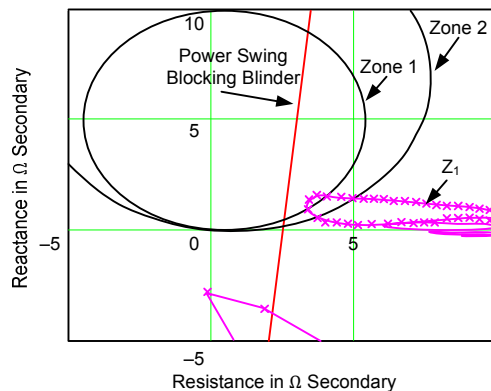


Fig. 9. Impedance plane plot of a high-load PSB scheme.

C. Nonconventional Power Swing Detection Methods

1) Continuous Impedance Calculation

The continuous impedance calculation consists of monitoring the progression in the complex plane (Fig. 10) of three modified loop impedances [7]. A power swing is declared when the criteria for all three loop impedances have been fulfilled: continuity, monotony, and smoothness. Continuity verifies that the trajectory is not motionless and requires that the successive ΔR and ΔX be above a threshold. Monotony verifies that the trajectory does not change direction by checking that the successive ΔR and ΔX have the same signs. Finally, smoothness verifies that there are no abrupt changes in the trajectory by looking at the ratios of the successive ΔR and ΔX that must be below some threshold.

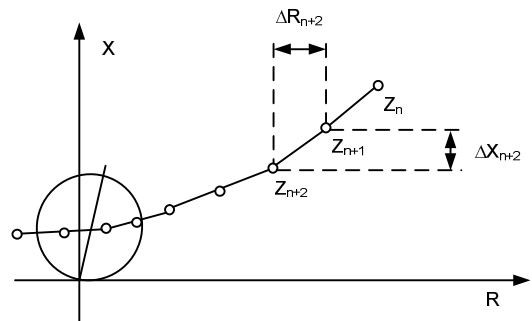


Fig. 10. Continuous impedance calculation.

The continuous impedance calculation is supplemented by a concentric characteristic to detect very slow-moving trajectories.

One of the advantages of the continuous impedance calculation is that it does not require any settings and can handle slip frequencies up to 7 Hz. It does not require, therefore, any power swing studies involving complex simulations.

2) Continuous Calculation of Incremental Current

During a power swing, both the phase voltages and currents undergo magnitude variations. The continuous calculation of the incremental current method computes the difference between the present current sample value and the value stored in a buffer 2 cycles before (see Fig. 11). The condition to declare a power swing is when the absolute value of the measured incremental current is greater than 5 percent of the nominal current and this same condition is present for a duration of 3 cycles [8].

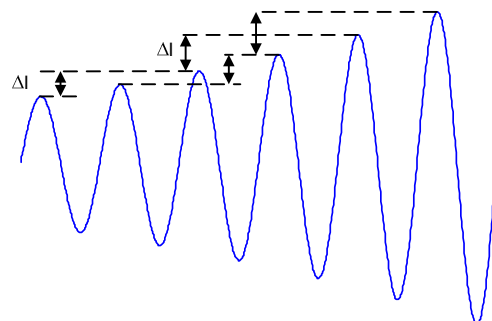


Fig. 11. Continuous calculation of incremental ΔI .

The main advantage of the continuous calculation of incremental current is that it can detect very fast power swings, particularly for heavy load conditions.

3) Synchrophasor-Based OOS Relaying

Consider the two-source equivalent network of Fig. 1, and assume that the synchrophasors of the positive-sequence voltages are measured at the left and right buses as V_{IS} and V_{IR} . The ratio of the two synchronized vectors is provided by the following equation:

$$\frac{V_{IS}}{V_{IR}} = \frac{\frac{Z_S}{Z_T} + (1 - \frac{Z_S}{Z_T}) \cdot k_E \angle \theta}{\frac{Z_S + Z_L}{Z_T} + (1 - \frac{Z_S + Z_L}{Z_T}) \cdot k_E \angle \theta} \quad (10)$$

where:

k_E is the ratio of the magnitudes of the source voltages:

$$k_E = \frac{|E_S|}{|E_R|} \quad (11)$$

Assuming the source impedances are small with respect to the line impedance and the ratio k_E is close to 1, the ratio of the synchronized vectors can be approximated by unity for its magnitude and by the angle θ between the two sources for its phase angle. As an example, assume the following:

$$\begin{aligned} k_E &= 1 \\ Z_S &= Z_R = j0.01\Omega \\ Z_L &= j0.1\Omega \end{aligned} \quad (12)$$

We then end up with the following equation for the vector ratio:

$$\frac{V_{IS}}{V_{IR}} = \frac{0.083 + 0.917\angle\theta}{0.917 + 0.083\angle\theta} \cong 1\angle\theta \quad (13)$$

When using the two-source network equivalent, the result of (13) indicates that the ratio of the synchrophasors measured at the line extremities has a phase angle that can be approximated by the phase angle between the two sources. During a disturbance, the trajectory of the phase angle between the two phasors replicates the variation of the phase angle between the two machines. It is therefore possible to determine if an OOS condition is taking place when the measured phase angle trajectory becomes unstable [9].

Following the same line of thinking, [10] presents an OOS detection system that measures the positive-sequence voltage phasors at two or more strategically located buses on the network. During a disturbance, the phase angle between the signal pairs is computed in real time, and a predictive algorithm is used to establish whether the disturbance will be

stable. A mathematical model of the phase angle time waveform is defined as an exponentially damped sine wave:

$$\delta(t) = \delta_0 + A \cdot e^{\alpha t} \cdot \sin(\omega t + \beta) \quad (14)$$

where:

δ_0 is the initial phase difference.

α is a damping constant.

ω is the angular frequency of the phase difference.

β is the phase shift.

A is the oscillation amplitude.

A predictive algorithm is used to identify the phase angle variation parameters and to determine stable or unstable conditions.

More recently, [11] presents the implementation of three functions based on synchrophasor measurements, the purpose of which is to trigger a network separation after a loss of synchronism has been detected. Positive-sequence voltage-based synchrophasors are measured at two locations of the network, assuming that the two-source equivalent can model the network. Following the measurement of the synchrophasors, two quantities are derived: the slip frequency S_R , which is the rate of change of the angle between the two measurements, and the acceleration A_R , which is the rate of change of the slip frequency. The three functions are defined as follows:

- Power swing detection is asserted when S_R is not zero and is increasing, which indicates A_R is positive and increasing.
- Predictive OST is asserted when, in the slip frequency against the acceleration plane, the trajectory falls in the unstable region (see Fig. 12) defined by the condition:

$$A_R > 78_Slope \cdot S_R + A_{Offset} \quad (15)$$

- OOS detection asserts when the absolute value of the angle difference between the two synchrophasors becomes greater than a threshold.

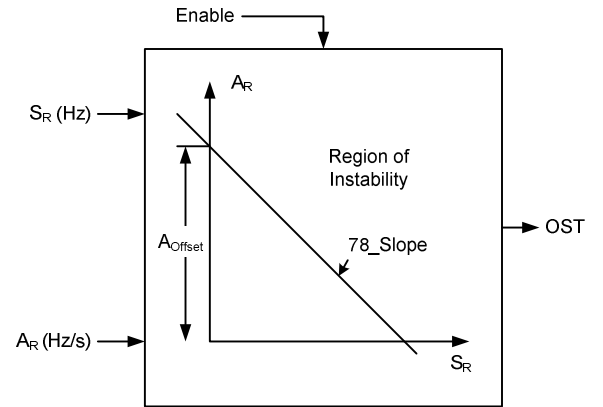


Fig. 12. Predictive OST in the slip-acceleration plane.

A network separation or OST is initiated when the three functions are asserted.

4) R-Rdot OOS Scheme

The R-Rdot relay for OST was devised specifically for the Pacific 500 kV ac intertie and was installed in the early 1980s. The R-Rdot relay uses the rate of change of resistance to detect an OOS condition.

An impedance-based control law for OOS detection is created by defining the following function [12] [13]:

$$U_1 = (Z - Z_1) + T_1 \cdot \frac{dZ}{dt} \quad (16)$$

where:

U_1 is the control variable.

Z is the apparent impedance magnitude at the relay.

Z_1 and T_1 are two settings that are derived from system studies; Z_1 is the impedance of the swing that is to be tripped, and T_1 is the slope that represents Rdot/R.

If we remove the impedance magnitude derivative term from (16), an OOS trip is initiated when Z becomes smaller than Z_1 or when U_1 becomes negative.

If we define a phase plane where the abscissa is the impedance magnitude and the ordinate is the rate of change of the impedance magnitude, (17) represents a switching line. An OOS trip is initiated when the switching line is crossed by the impedance trajectory from right to left. The effect of adding the impedance magnitude derivative is that the tripping will be faster at a higher impedance changing rate. At a small impedance changing rate, the characteristic is equivalent to the conventional OOS scheme.

$$U_1 = (R - R_1) + T_1 \cdot \frac{dR}{dt} \quad (17)$$

In the R-Rdot characteristic, the impedance magnitude is replaced by the resistance measured at the relay and the rate of change of the impedance magnitude is replaced by the rate of change of the measured resistance.

The advantage of this latter modification is that the relay becomes less sensitive to the location of the swing center with respect to the relay location.

More than one control law can be implemented in a relay so that multiple switching lines can be implemented, depending upon what is needed. For a conventional OST relay without a rate of change of apparent resistance, augmentation is just a vertical line in the R-Rdot plane offset by the R_1 relay setting parameter. The switching line U_1 is a straight line having slope T_1 in the R-Rdot plane. System separation is initiated when output U_1 becomes negative. For low separation rates (small dR/dt), the performance of the R-Rdot scheme is similar to the conventional OST relaying schemes. However, higher separation rates (dR/dt) would cause a larger negative value of U_1 and initiate tripping much earlier. In the actual implementation, the relay uses a piecewise linear characteristic consisting of two line segments rather than the straight line shown in Fig. 13.

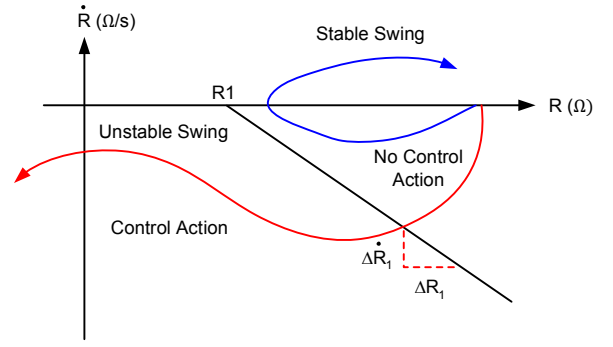


Fig. 13. R-Rdot OOS characteristic in the phase plane.

5) Rate of Change of Swing Center Voltage

SCV is defined as the voltage at the location of a two-source equivalent system where the voltage value is zero when the angles between the two sources are 180 degrees apart (see Fig. 2). Fig. 14 illustrates the voltage phasor diagram of a general two-source system, with the SCV shown as the phasor from origin o to the point o' .

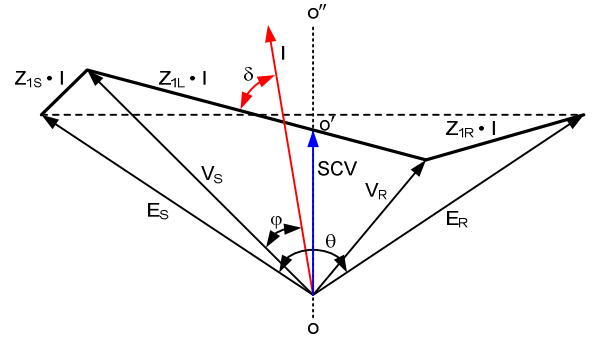


Fig. 14. Voltage phasor diagram of a two-source system.

When a two-source system loses stability and enters an OOS condition, the angle difference of the two sources, $\theta(t)$, increases as a function of time. As derived in detail in [3], we can represent the SCV with (18), assuming an equal source magnitude, $E = |E_S| = |E_R|$.

$$SCV(t) = \sqrt{2}E \sin\left(\omega t + \frac{\theta(t)}{2}\right) \cdot \cos\left(\frac{\theta(t)}{2}\right) \quad (18)$$

$SCV(t)$ is the instantaneous SCV that is to be differentiated from the SCV that the relay estimates. Equation (18) is a typical amplitude-modulated sinusoidal waveform. The first sine term is the base sinusoidal wave, or the carrier, with an average frequency of $\omega + (1/2)(d\theta/dt)$. The second term is the cosine amplitude modulation.

Fig. 15 shows a positive-sequence SCV (SCV1) for a power system with a nominal frequency of 50 Hz and a constant slip frequency of 5 Hz. When the frequency of a sinusoidal input is different from that assumed in its phasor calculation, as in the case of an OOS situation, oscillations in the phasor magnitude result. However, the amplitude calculation in Fig. 15 is smooth because the positive-sequence quantity effectively averages out the amplitude oscillations of individual phases.

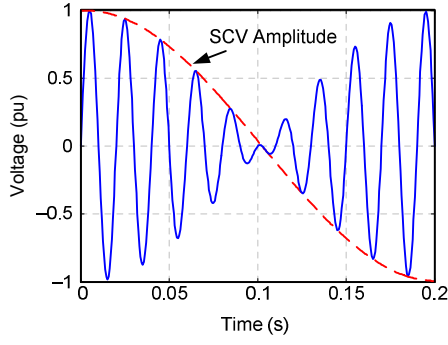


Fig. 15. SCV during an OOS condition.

The magnitude of the SCV changes between 0 and 1 per unit of system nominal voltage. With a slip frequency of 5 Hz, the voltage magnitude is forced to 0 every 0.2 seconds. Fig. 15 shows the SCV during a system OOS condition. Under normal load conditions, the magnitude of the SCV stays constant.

One popular approximation of the SCV obtained through the use of locally available quantities is as follows:

$$\text{SCV} \approx |V_S| \cdot \cos \varphi \quad (19)$$

where:

$|V_S|$ is the magnitude of locally measured voltage.
 φ is the angle difference between V_S and the local current, as shown in Fig. 16.

The quantity of $V \cos \varphi$ was first introduced by Ilar for the detection of power swings [14].

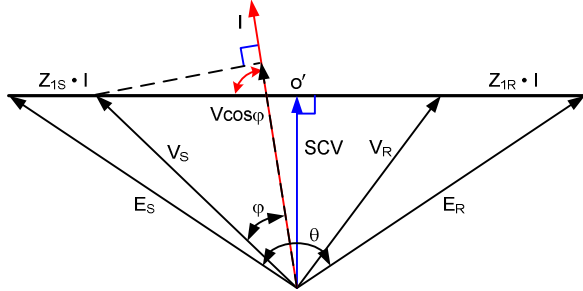


Fig. 16. $V \cos \varphi$ is a projection of local voltage, V_S , onto local current, I .

In Fig. 16, we can see that $V \cos \varphi$ is a projection of V_S onto the axis of the current, I . For a homogeneous system with the system impedance angles close to 90 degrees, $V \cos \varphi$ approximates well the magnitude of the SCV. For the purpose of power swing detection, it is the rate of change of the SCV that provides the main information of system swings. Therefore, some difference in magnitude between the system SCV and its local estimate has little impact in detecting power swings. We will, therefore, refer to $V \cos \varphi$ as the SCV in the following discussion.

Using (18) and keeping in mind that the local SCV is estimated using the magnitude of the local voltage, V_S , the relation between the SCV and the phase angle difference, θ , of two source voltage phasors can be simplified to the following:

$$\text{SCV1} = E_1 \cdot \cos\left(\frac{\theta}{2}\right) \quad (20)$$

In (20), E_1 is the positive-sequence magnitude of the source voltage, E_S , shown in Fig. 16 and is assumed to be also equal to E_R . We use SCV1 in power swing detection for the benefit of its smooth amplitude during a power swing on the system. The magnitude of the SCV is at its maximum when the angular difference between the two sources is zero. Conversely, it is at its minimum (or zero) when the angular difference between the two sources is 180 degrees. This property has been exploited so that a power swing can be detected by calculating the rate of change of the SCV. The time derivative of SCV1 is given by (21).

$$\frac{d(\text{SCV1})}{dt} = -\frac{E_1}{2} \sin\left(\frac{\theta}{2}\right) \frac{d\theta}{dt} \quad (21)$$

Equation (21) provides the relationship between the rate of change of the SCV and the two-machine system slip frequency, $d\theta/dt$. Equation (21) shows that the derivative of SCV1 is independent of power system impedances. Fig. 17 is a plot of SCV1 and the rate of change of SCV1 for a system with a constant slip frequency of 1 radian per second.

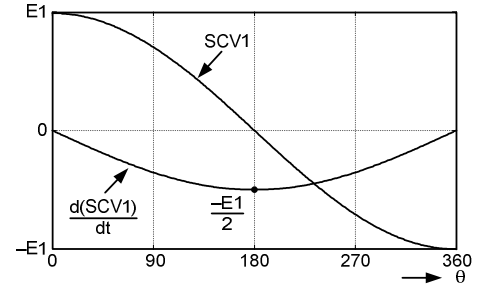


Fig. 17. SCV1 and its rate of change with unity source voltage magnitudes.

Before ending this section, we want to point out the following two differences between the system SCV and its local estimate:

1. When there is no load flowing on a transmission line, the current from a line terminal is basically the line charging current that leads the local terminal voltage by approximately 90 degrees. In this case, the local estimate of the SCV is close to zero and does not represent the true system SCV.
2. The local estimate of the SCV has a sign change in its value when the difference angle, θ , of two equivalent sources goes through 0 degrees. This sign change results from the reversal of the line current (i.e., φ changes 180 degrees when θ goes through the 0-degree point). The system SCV does not have this discontinuity.

IV. PSB COMPARISON BETWEEN DUAL-QUADRILATERAL AND SCV METHODS

A. Simulation Examples of Power Swing Detection

In this section, we compare the performance of the dual-quadrilateral method with that of the SCV. The two methods operate on different principles but ultimately arrive at the same result. This section presents a comparison of the two methods as they apply to an equivalent two-source power

system. The power system used for the comparison consists of two strong sources connected through a parallel transmission line (see Fig. 18). The power system is built in an RTDS environment. The simulated data are played back to a relay having either the dual-quadrilateral or the SCV PSB method enabled.

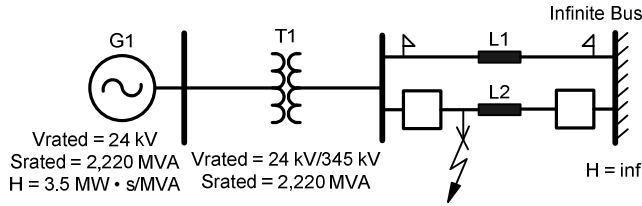


Fig. 18. Power system simulation model.

To create the power swing, a three-phase fault is placed on Line L2 close in to the bus but cleared after a set delay. The fault and the delay of the fault clearing cause the power swing and also determine if the swing will be stable or unstable. The power swing is monitored on Line L1 at the left relay flag indicator in Fig. 18, while the breakers are open on Line L2. Reclosing is also implemented to close L2 back into service 1 second after the breakers are tripped. Reclosing does not impact the operation of the PSB detection. When the previously faulted line is switched back into service, the line immediately picks up load, thereby reducing load current in the unfaulted line. This appears as an increase in impedance when viewed from the unfaulted line. However, from the point of view of the power system, the overall impedance is decreased (the two lines are now once again in parallel) and the power transfer capability of the system is increased, thereby increasing the generator stability.

To test the operation of both PSB detection methods, stable and unstable swings are produced from the simulation. The generator in the simulation model is equipped with both an automatic voltage regulator and a power system stabilizer, but for the cases presented here, both are turned off.

For a stable swing, the swing rate is approximately 1.2 Hz (see Fig. 19). The positive-sequence impedance for the stable swing is shown in Fig. 20. At 100 cycles, L2 is reclosed. When L2 is closed back in, the L1 current decreases because L2 carries half of the load. This appears as an increase of impedance on the relay that monitors L1 voltages and currents.

The unstable swing is about 4.5 Hz with an increasing swing rate of up to 8.5 Hz (see Fig. 21). The positive-sequence impedance for the unstable swing is plotted in Fig. 22. Similar to the stable swing, the reclosing occurs at 100 cycles, decreasing the system impedance and increasing power transfer capability. Both of these simulation cases are saved as Common Format for Transient Data Exchange (COMTRADE) files and played back to the relay through a test set to see how the PSB logic will behave.

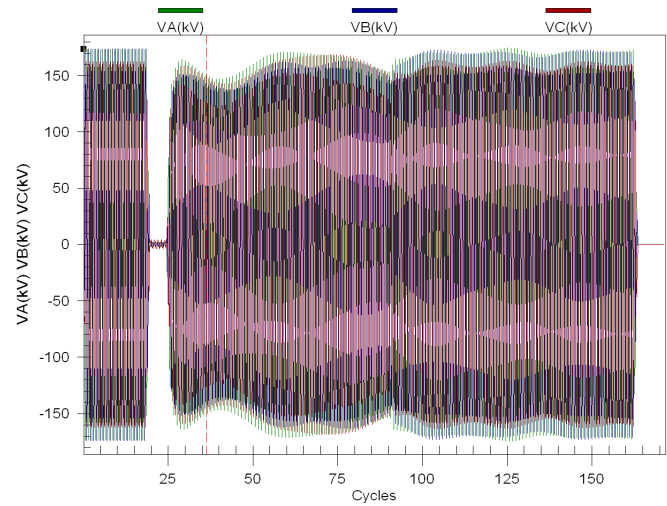


Fig. 19. Stable power swing.

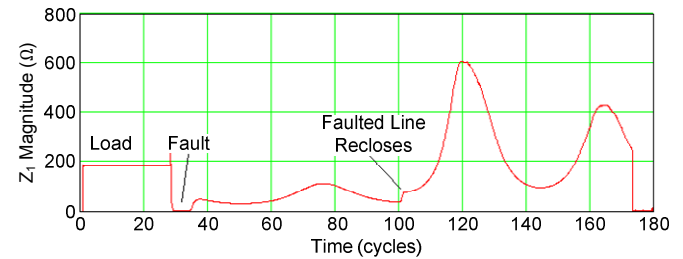


Fig. 20. Z_1 impedance magnitude plot for the stable power swing.

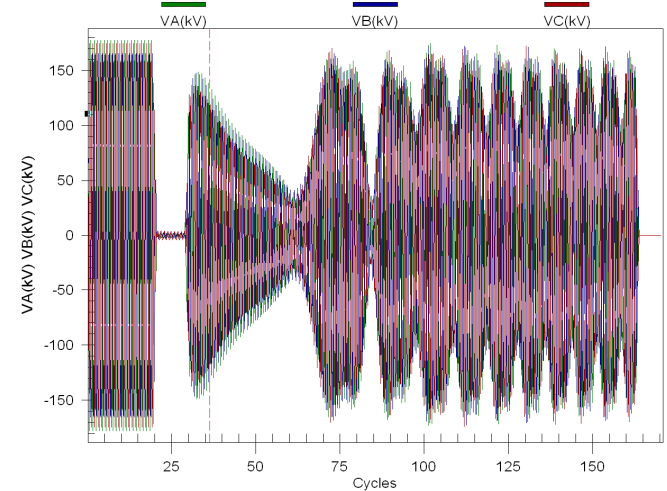


Fig. 21. Unstable power swing.

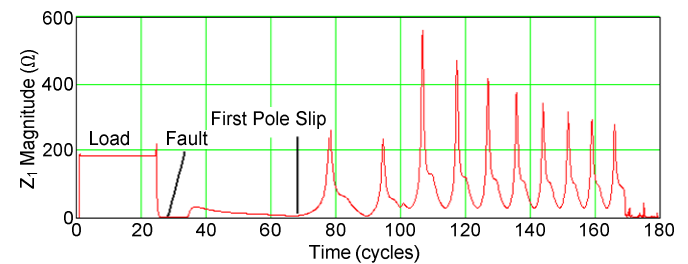


Fig. 22. Impedance plot for the unstable power swing.

The system parameters that are needed to make settings calculations are shown in Table I.

TABLE I
POWER SYSTEM SIMULATION MODEL DETAILS

Parameter	Value
L1 positive-sequence impedance (Ω secondary)	$18.86 \angle 87.19^\circ \Omega$
Relay current transformer ratio	3000:1
Relay voltage transformer ratio	3000:1
Load impedance	180Ω
Stable swing rate	1.2 Hz
Unstable swing rate	4.5 to 8.5 Hz

The system is protected by three mho elements, where Zones 1 and 2 are forward and Zone 3 is reverse. Zone 1 is set at 80 percent of the line impedance, or 15.08Ω , and Zone 2 is set at 120 percent of the line impedance, or 22.62Ω .

The quadrilateral inner and outer blinders are selected with a few observations. First, the load must be considered. If the outer blinder is set too large and encroaches on the load, the PSB function will be in danger of operating during heavy load conditions. Second, the inner blinder must be set larger than the Zone 1 and Zone 2 and possibly larger than the Zone 4 mho elements that are supervised by the PSB element. Finally, the two blinders must be far enough apart to allow enough time to capture the fastest swing rate determined from the system study. The selection of the two impedances for the inner and outer blinders for this simulation meets all three criteria (see Fig. 23).

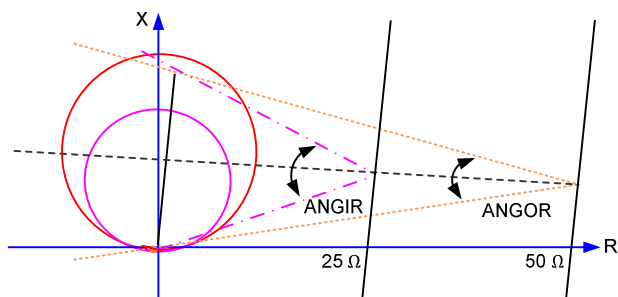


Fig. 23. Dual-quadrilateral settings calculation.

From the equations in [6], the angle of the inner radius, ANGIR, and the angle of the outer radius, ANGOR, can be calculated. For this simulation, the inner radius and outer radius are 41 degrees and 21 degrees, respectively.

Next, the PSB delay is calculated and verified using the equation from [6]. The blocking delay is typically set from 1.5 to 2.5 cycles to give the relay a greater ability to detect the difference between a fault and an OOS condition [6]. The simulation uses a PSB delay of 0.61 cycles, or 10 milliseconds, to detect and block for an unstable swing that

has a rate of approximately 5.5 Hz. The subcycle PSB delay was selected for demonstration purposes only. The relay has a processing interval of 2 milliseconds.

There are no settings associated with the SCV variation method; therefore, it does not require any power system studies in order to be applied properly.

The first simulation is a stable power swing for the dual-quadrilateral method. Fig. 24 shows the stable power swing and the PSB elements asserting as the impedance passes through the inner and outer blinders, X6ABC and X7ABC, set at 25Ω and 50Ω , respectively. It also shows that Z3P asserts for a short period of time because the fault is seen as behind this relay.

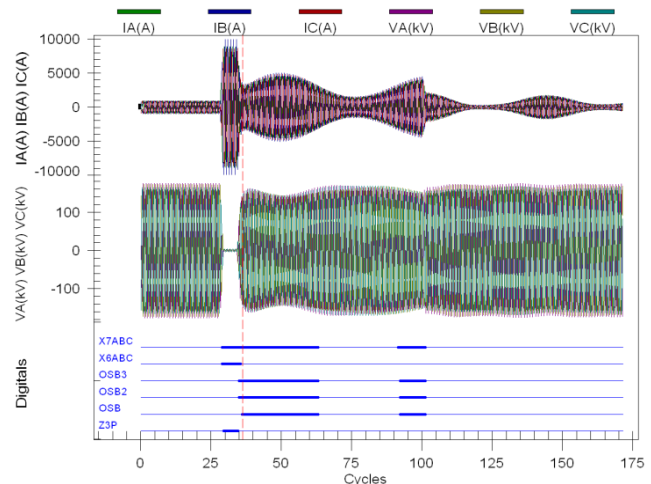


Fig. 24. Stable swing using the dual-quadrilateral technique.

The results of the simulation for the SCV PSB method are shown in Fig. 25, Fig. 26, and Fig. 27. Both techniques detect the power swing condition and block accordingly.

The SCV method for detecting a power swing is slower than the dual-quadrilateral method. This is seen by comparing Fig. 24 with Fig. 25. It is slower because of the slow rate of change of the SCV. This is confirmed when studying Fig. 26.

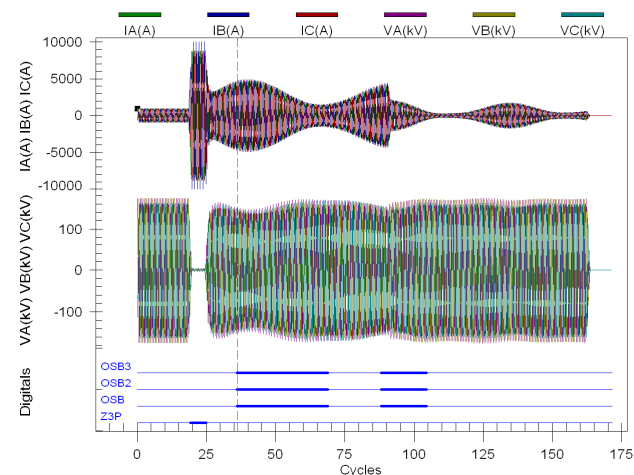


Fig. 25. Stable swing using the SCV technique.

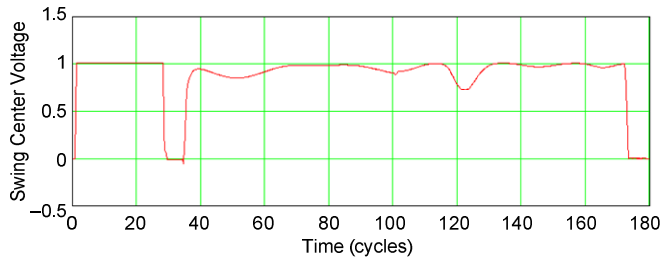


Fig. 26. SCV magnitude during the stable swing.

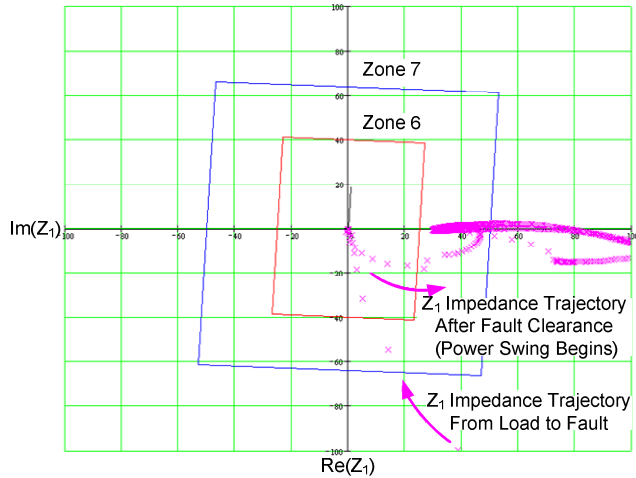


Fig. 27. Impedance plot of the stable power swing condition.

The final simulations apply an unstable swing with an initial swing rate of 4.5 Hz and verify that the two methods operate similarly. Because the system was not set up for OST, the simulation focuses on the assertion of the PSB elements. The results of the unstable power swing using the dual-quadrilateral technique are shown in Fig. 28.

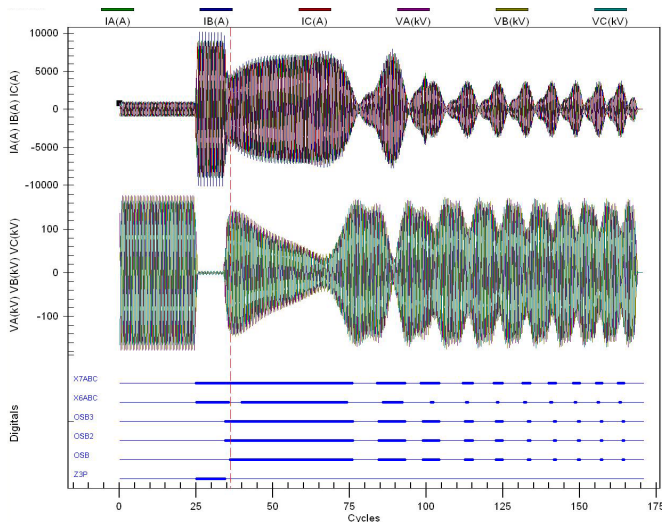


Fig. 28. Unstable swing using the dual-quadrilateral technique.

Fig. 29, Fig. 30, and Fig. 31 show the results from the unstable power swing using the SCV method. Again, both techniques detect the power swing condition in about the same amount of time.

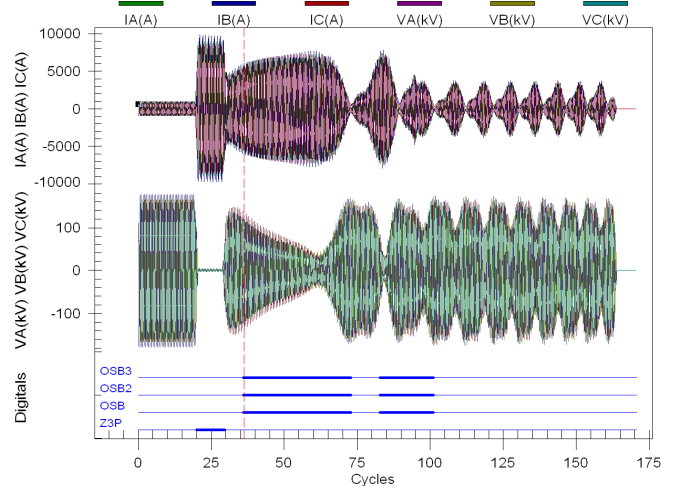


Fig. 29. Unstable swing using the SCV variation technique.

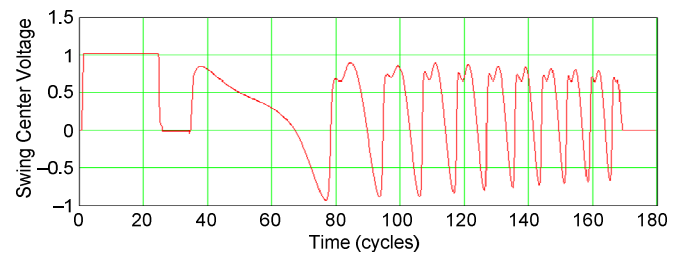


Fig. 30. SCV magnitude during the unstable swing.

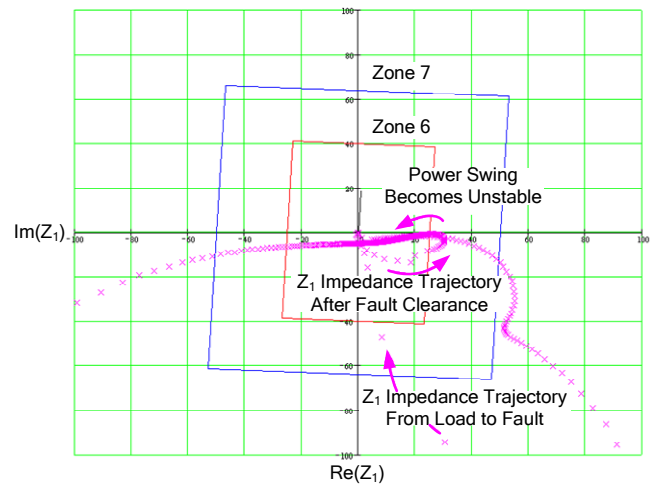


Fig. 31. Impedance plot of the unstable power swing condition.

B. Comparison Using Field Events

1) Example 1

The first field event relates to a substantial power swing that took place on the network of a South American country in January 2005 and lasted for about 2 seconds. The event report ER 1 was recorded by the relay protecting a 76.67-kilometer 120 kV transmission line with the following secondary impedance characteristics:

$$Z_1 = 2.05 \angle 71^\circ \Omega$$

$$Z_0 = 6.77 \angle 72^\circ \Omega$$

The line was protected by four mho elements covering Zones 1 through 4. Zones 2 and 3 were used in a directional comparison blocking (DCB) communications scheme. Zones 6 and 7 (quadrilateral blinders) were used for PSB detection following the principles of the dual-quadrilateral method. The minimum PSB delay to cross from Zone 7 to Zone 6 had been set at 2 cycles.

Fig. 32 shows the line voltages and currents recorded by ER 1 during the power swing. Fig. 33 shows the Z_1 impedance trajectory during the power swing.

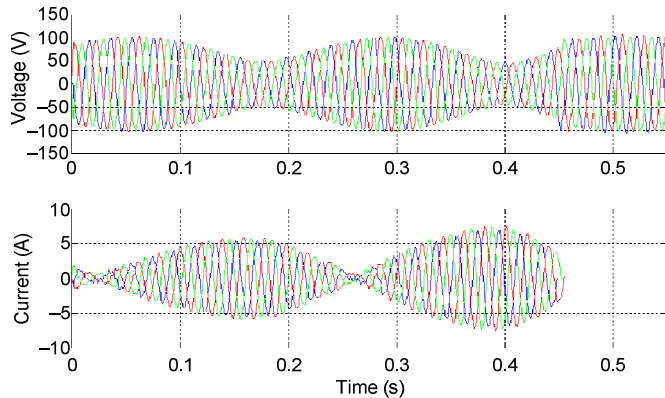


Fig. 32. Phase voltages and currents during the power swing for ER 1.

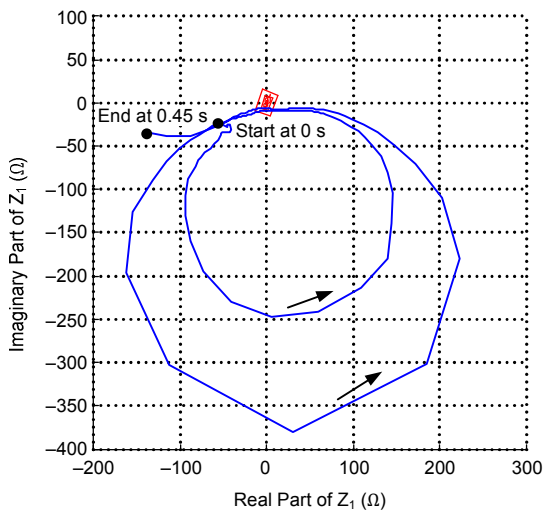


Fig. 33. Trajectory of Z_1 in the complex plane for ER 1.

Looking at Fig. 34, which shows the Z_1 trajectory crossing Zones 7 and 6, we can see that during the first crossing, the locus of Z_1 stayed in Zone 7 for 25 milliseconds (0.179 minus 0.154 seconds). Because the PSB delay was set to 2 cycles, the power swing could not be detected during the first crossing. During the second crossing of Zone 7, the Z_1 locus stayed in Zone 7 for 26 milliseconds (0.397 minus 0.371 seconds). Again, the power swing could not be detected, for the same reason. This example is therefore the classical situation where the speed of the Z_1 trajectory was not taken into account in the choice of the time settings.

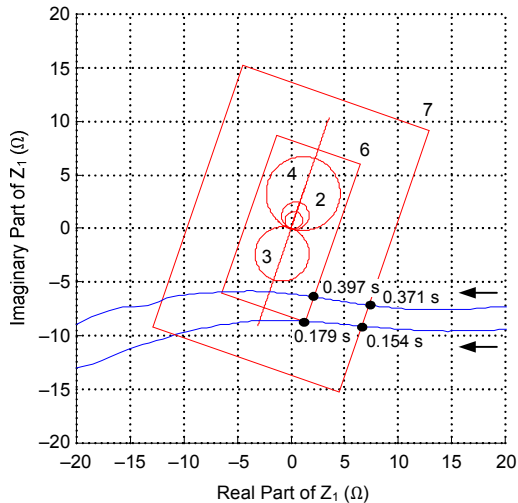


Fig. 34. Trajectory of Z_1 across Zones 6 and 7 for ER 1.

In order to be able to detect this OOS condition, the solution is to expand Zone 7 so as to broaden the corridor between Zone 7 and Zone 6 and then provide more time to the Z_1 locus to stay inside Zone 7. Another solution would be to shorten the time delay for detecting the OOS condition, if possible.

Fig. 35 displays the PSB and mho element logic signals when the data were processed through a mathematical model of the relay that used the dual-quadrilateral technique. Because the power swing had not been detected, Zones 1, 2, and 4 (M1P, M2P, and M4P) operated during the event.

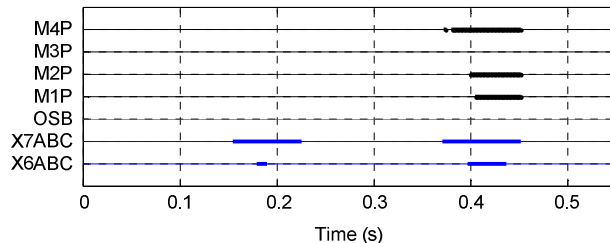


Fig. 35. OOS and phase mho logic signals for ER 1 (dual-quadrilateral method).

Observe from Fig. 33 and Fig. 34 that the trajectory of the positive-sequence impedance did not traverse the forward-looking Zone 1, 2, or 4 distance elements. So why did these elements operate? The reason for their operation has to do with how these elements are polarized. The distance elements are polarized using positive-sequence memory voltage. The stiffness of the memory voltage is responsible for the assertion of forward-looking distance elements. In short, the frequency of the memory voltage polarizing signal and that of the operating signal do not correspond, resulting in the operation of the forward elements.

The event data were then processed by a mathematical model of the relay that uses the SCV technique. Fig. 36 shows the Z_1 trajectory entering the start zone. Because there is no delay in the SCV method associated with the crossing of the start zone, as shown in Fig. 37, the power swing detection signal will assert as soon as the start zone is crossed.

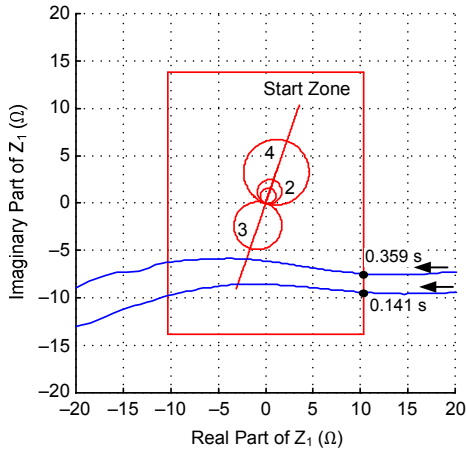


Fig. 36. Trajectory of Z_1 with respect to the start zone for ER 1 (SCV method).

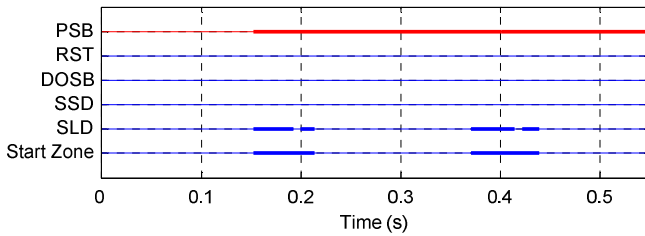


Fig. 37. OOS logic signals for ER 1 (SCV method).

Fig. 38 shows the SCV1 together with the magnitude of the positive-sequence voltage. As shown in Fig. 37, the power swing is detected by the slope detector as soon as the Z_1 locus crosses the start zone. Had the SCV method been used in the original application, the line trip would have been avoided.

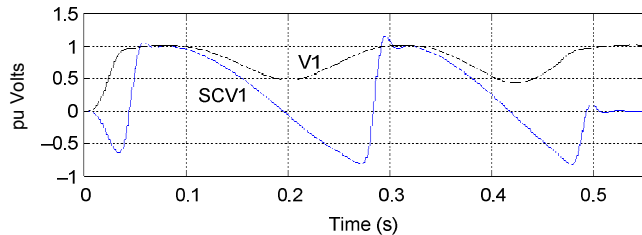


Fig. 38. Positive-sequence voltage magnitude and SCV1 for ER 1.

2) Example 2

The second field event is from the same network as the first event and happened on the same day during the same power swing. The event report ER 2 was recorded by the relay protecting the adjacent 182.17-kilometer line and at the same voltage level as before, 120 kV. The line had the following secondary impedance characteristics:

$$Z_1 = 4.87 \angle 71.2^\circ \Omega$$

$$Z_0 = 16.08 \angle 72.26^\circ \Omega$$

The line had the same protection scheme as in the previous example.

Fig. 39 shows the line voltages and currents recorded by ER 2 during the power swing. Fig. 40 shows the Z_1 impedance trajectory during the power swing.

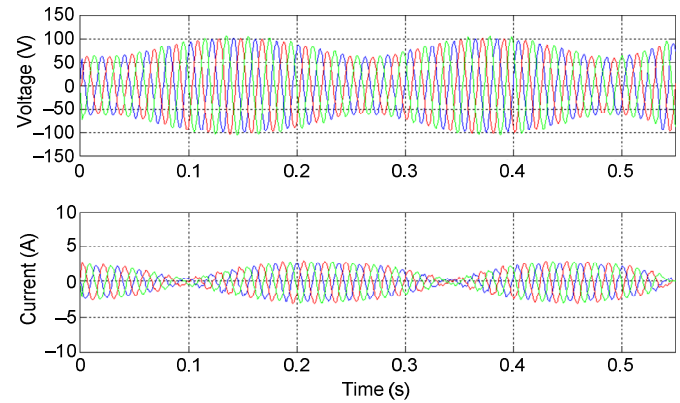


Fig. 39. Phase voltages and currents during the power swing for ER 2.

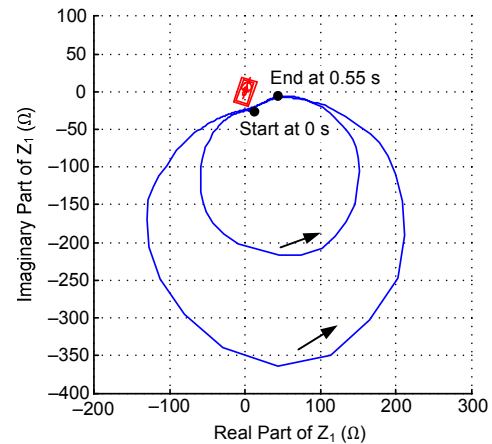


Fig. 40. Trajectory of Z_1 in the complex plane for ER 2.

Looking at Fig. 41, we can see that the Z_1 trajectory simply did not cross Zones 7 or 6. It is therefore impossible in this case to detect the power swing with the dual-quadrilateral method and the settings selected by the user in the first place.

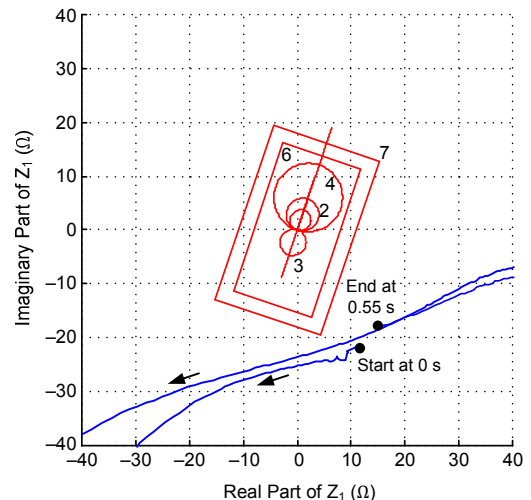


Fig. 41. Trajectory of Z_1 across Zones 6 and 7 for ER 2.

Fig. 42 displays the OOS and mho distance elements. From this, we can deduce that the mho phase distance element for Zones 1, 2, and 4 asserted during the power swing.

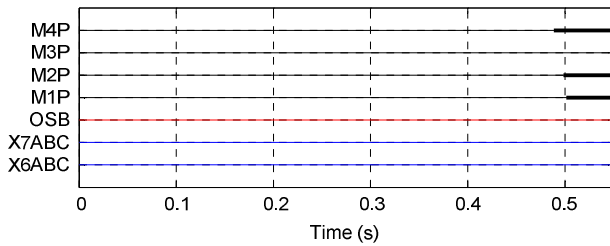


Fig. 42. OOS and phase mho logic signals for ER 2 (dual-quadrilateral method).

In the same way as the previous example, the voltage and current waveforms were processed by a mathematical model implementing the SCV method. Fig. 43 shows the Z_1 trajectory entering the start zone. The crossing occurs at 0.24 seconds. The power swing detection signal will assert as soon as the start zone has been crossed.

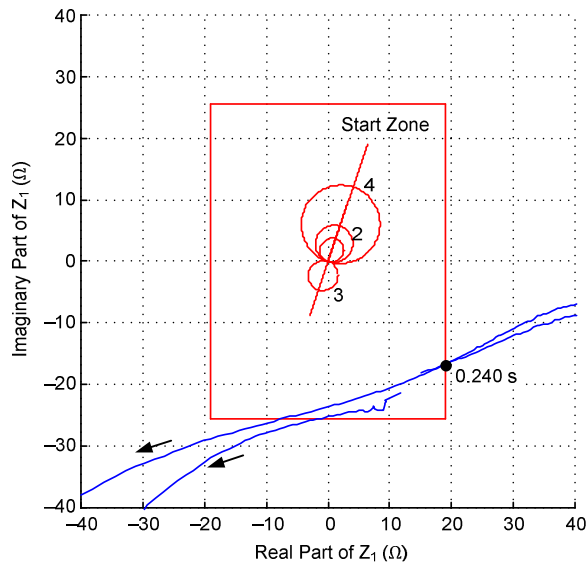


Fig. 43. Trajectory of Z_1 with respect to the start zone for ER 2 (SCV method).

Fig. 44 shows the SCV1 together with the magnitude of the positive-sequence voltage during the power swing. As shown in Fig. 45, the power swing is detected by the slope detector as soon as the Z_1 locus crosses the start zone. As in the previous example, if the SCV method had been used, the line trip would have been avoided.

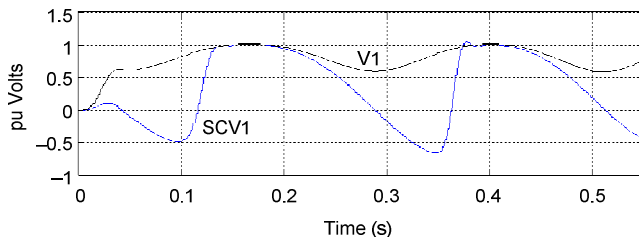


Fig. 44. Positive-sequence voltage magnitude and SCV1 for ER 2.

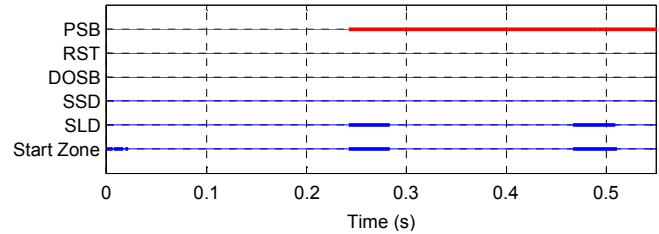


Fig. 45. OOS logic signals for ER 2 (SCV method).

These two examples illustrate that the SCV method is more appropriate for fast power swings and would reliably declare a power swing condition, even under unusual swing speeds.

V. OUT-OF-STEP TRIPPING

The function of OST schemes is to protect the power system during unstable conditions by isolating unstable generators or larger power system areas from each other by forming system islands. The main criterion is to maintain stability within each island. To accomplish this, OST systems should be applied at preselected network locations, typically near the network electrical center, to achieve a controlled system separation. Separation should take place at such points in the network to preserve a close balance between load and generation. Where a load-generation balance cannot be achieved, some means of shedding load or generation should take place to avoid a complete shutdown of the power system.

OST systems must be complemented with PSB functions to prevent undesired relay system operations, equipment damage, and the shutdown of major portions of the power system. In addition, PSB blocking should be applied at other network locations to prevent system separation in an indiscriminate manner.

The selection of network locations for the placement of OST systems can best be obtained through transient stability studies covering many possible operating conditions. The maximum rate of slip is typically estimated from angular change versus time plots from stability studies. The stability study results are also used to identify the optimal location of OST and PSB relay systems, because the apparent impedance measured by OOS relay elements is a function of the MW and MVAR flows in transmission lines. Stability studies help identify the parts of the power system that impose limits on angular stability, generators that are prone to go out of step during system disturbances and those that remain stable, and groups of generators that tend to behave similarly during a disturbance [15].

Typically, the location of OST relay systems determines the location where system islanding takes place during loss of synchronism. However, in some systems, it may be necessary to separate the network at a location other than the one where OST is installed. This is accomplished with the application of a transfer tripping scheme. Current supervision may be necessary when performing OST at a different power system location than the location of OST detection to avoid issuing a tripping command to a circuit breaker at an unfavorable phase

angle. Another important aspect of OST is to avoid tripping a line when the angle between systems is near 180 degrees. Tripping during this condition imposes high stresses on the breaker and could cause breaker damage as a result of high recovery voltage across the breaker contacts, unless the breaker is rated for out-of-phase switching [16].

A. Conventional OST Schemes

Conventional OST schemes are based on the rate of change of the measured positive-sequence impedance vector during a power swing. The OST function is designed to differentiate between a stable and an unstable power swing and, if the power swing is unstable, to send a tripping command at the appropriate time to trip the line breakers. Traditional OST schemes use distance characteristics similar to the PSB schemes shown in Fig. 5, Fig. 6, and Fig. 7. OST schemes also use a timer to time how long it takes for the measured impedance to travel between the two concentric characteristics. If the timer expires before the measured impedance vector travels between the two characteristics, the relay declares the power swing as an unstable swing and issues a tripping signal.

Fig. 7 shows the dual-quadrilateral characteristic used for the detection of power swings. When the positive-sequence impedance enters the outer zone, two OOS logic timers start (OSTD and OSBD). Fig. 46 illustrates how these timers operate.

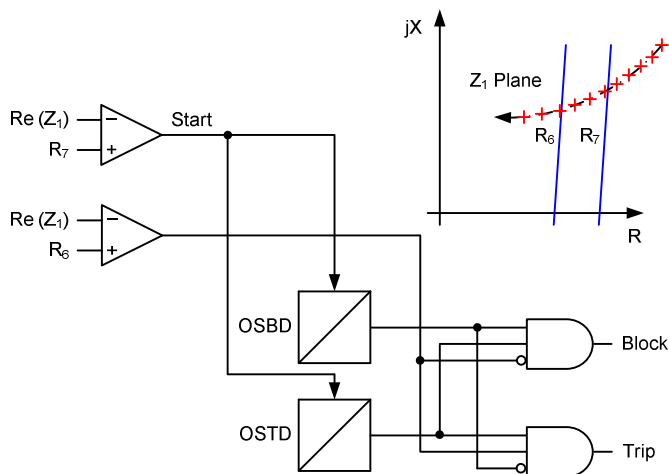


Fig. 46. Dual-quadrilateral timer scheme.

There are two methods to implement out-of-step tripping. The first method is to select to trip on the way in (TOWI) when the OSTD timer expires and the positive-sequence impedance enters the inner zone. The second method is to select to trip on the way out (TOWO) when the OSTD timer expires and the positive-sequence impedance enters and then exits the inner zone. TOWO is the most desirable method because it allows tripping of the breaker to take place in a more favorable time, during the slip cycle when the two systems are close to an in-phase condition. The term *way out* refers to the impedance trajectory seen by the relay and the

point at which OST is initiated (on the way out of the operating region of the inner OST characteristic). Note that in some other implementations, TOWO takes place when the positive-sequence impedance exits the outer OST characteristic.

Stability studies in some large, interconnected power systems in North America have revealed that delaying OST until the relative phase angle of the two systems reaches 270 degrees can cause instability in subnetworks within each utility system. Therefore, TOWO was not deemed to be fast enough, and new requirements were imposed on relay manufacturers to develop OST schemes that allow systems to trip before they reach a relative phase angle of 90 degrees. This is referred to as TOWI. The term *way in* refers to the impedance trajectory seen by the relay and the point at which OST is initiated (on the way into the operating region of the inner OST characteristic).

TOWI is useful in some systems to prevent severe voltage dips and potential loss of loads. TOWI is typically applied in very large systems where the angular movement of one system with respect to another is very slow. It is also applied where there is a real danger that transmission line thermal damage will occur if tripping is delayed until a more favorable angle exists between the two systems [3]. However, we should be careful because the relay issues the tripping command to the circuit breaker when the relative phase angles of the two systems approach 180 degrees, which results in greater breaker stress than for OST applications that implement TOWO.

One of the most important and difficult aspects of an OST scheme is the calculation of proper settings for the distance relay OST characteristics and the OST time-delay setting. We should be absolutely certain that a stable power swing never crosses the inner OST characteristic in order to avoid a system separation during a stable power swing from which the system can recover. In addition, we should determine the fastest unstable power swing. To determine these settings, we must run extensive stability studies and be certain that all possible system scenarios have been considered. As a general rule, the inner characteristic should be set anywhere between 120 and 150 degrees, making sure that the inner zone asserts only for an unstable power swing. On the other hand, the outer zone should be set away from the maximum expected line loading (typically near 80 to 90 degrees).

The other difficult aspect of OST schemes is determining the appropriate time at which to issue a trip signal to the line breakers to avoid equipment damage and ensure personnel safety. To adequately protect the circuit breakers and ensure personnel safety, most utilities do not allow uncontrolled tripping during an OOS condition by restricting the operation of OST relays when the relative voltage angle between the two systems is less than 90 degrees and greater than 270 degrees. Logic is included to allow delayed OST on the way out to minimize the possibility of breaker damage.

B. Application of Traditional OST Schemes

The recommended approach for traditional OST schemes is summarized as follows:

- Perform system transient stability studies to identify system stability constraints based on many operating conditions and stressed system operating scenarios. The stability studies help identify the parts of the power system that impose limits to angular stability, generators that are prone to go out of step during system disturbances and those that remain stable, and groups of generators that tend to behave similarly during a disturbance.
- Determine the locations of the swing loci during various system conditions, and identify the optimal locations to implement the OST protection function. The optimal location for the detection of the OOS condition is near the electrical center of the power system. However, we must determine that the behavior of the impedance locus near the electrical center would facilitate successful OOS detection.
- Determine the optimal location for system separation during an OOS condition. This typically depends on the impedance between islands, the potential to attain a good load-generation balance, and the ability to establish stable operating areas after separation. To limit the amount of generation and load shed in a particular island, it is essential that each island have reasonable generation capacity to balance the load demand. High-impedance paths between system areas typically represent appropriate locations for network separation.
- Establish the maximum rate of slip between systems for OOS timer setting requirements as well as the minimum forward and reverse reach settings required for successful detection of OOS conditions. The swing frequency of a particular power system area or group of generators relative to another power system area or group of generators does not remain constant. The dynamic response of generator control systems, such as automatic voltage regulators, and the dynamic behavior of loads or other power system devices, such as static VAR compensators and flexible ac transmission systems (FACTS), can influence the rate of change of the impedance measured by OOS protection devices.
- Set the OST inner zone at a point along the OOS swing trajectory where the power system cannot regain stability. Set the OST outer zone such that the minimum anticipated load impedance locus is outside the outermost zone. The OST time delay is set based on the settings of the inner and outer zone resistance blinders and the fastest OOS swing frequency expected or determined from transient stability studies.

C. Application of SCV Method

All of the previously discussed OST setting complexities and the need for stability studies can be eliminated if the OST function uses, as one of its inputs, the output of the robust SCV function that makes certain that the network is experiencing a power swing and not a fault. Using a reliable bit from the SCV function to supervise the SCV-assisted OST function allows us to implement TOWO without performing any stability studies, which is a major advantage over traditional OST schemes.

The SCV OST scheme tracks the positive-sequence impedance Z_1 trajectory as it moves throughout the complex plane. The SCV OST function tracks and verifies that the measured Z_1 impedance trajectory crosses the complex impedance plane from right to left, or from left to right, and issues a TOWO at a desired phase angle difference between sources. Verifying that the Z_1 impedance enters the complex impedance plane from the left or right side and making sure it exits at the opposite side of the complex impedance plane ensure that the function operates only for unstable power swings. On the contrary, traditional OST schemes that do not track the Z_1 impedance throughout the complex impedance plane may operate for a stable swing that was not considered during stability studies and happens to cross the inner OST characteristic.

Four resistive and four reactive blinders are still used in the SCV OST scheme, as shown in Fig. 7. However, the settings for these blinders are easy to calculate when applying TOWO. The outermost OST resistive blinders can be placed around 80 to 90 degrees in the complex impedance plane, regardless of whether a stable power swing crosses these blinders or whether the load impedance of a long, heavily loaded line encroaches upon them. The inner OST resistive blinder can be set anywhere from 120 to 150 degrees. In addition, there are no OST timer settings involved in the new SCV-assisted OST scheme. To apply TOWI, we still need to perform stability studies to ensure that no stable swings will cause the operation of the inner OST characteristic.

The SCV OST function offers the following three options:

- TOWO during the first slip cycle.
- TOWO after a set number of slip cycles has occurred.
- TOWI before completion of the first slip cycle.

VI. OST COMPARISON BETWEEN THE DUAL-QUADRILATERAL AND SCV METHODS

We conducted simulations to demonstrate how TOWI and TOWO operate differently with the dual-quadrilateral and SCV OST methods. We use the same simulations and settings from Section IV to show how the OST logic operates under the same conditions as the PSB logic. Both methods require setting the OST characteristic to provide an operating zone for the OST logic, as stated in Section IV. The settings for the OST blinders of the conventional dual-quadrilateral scheme are chosen by studying the impedance plots of stable and

unstable RTDS simulations. The settings for the SCV-assisted OST scheme are set without studying the trajectories from the RTDS simulations. It is also necessary to set a timer for the dual-quadrilateral OST algorithm. This timer is set to an average swing rate that is detected for unstable cases; there is no timer setting necessary for the SCV OST detection algorithm.

Fig. 47 through Fig. 50 show the response of the relay using both the dual-quadrilateral and the SCV techniques. Fig. 47 and Fig. 48 demonstrate TOWI and show that the OST bit asserted and tripped the relay before the first slip cycle. The relay tripped before the voltage dip became too severe, which is one of the reasons to use TOWI instead of TOWO. Observe that at the point where the relay trips using the TOWO method (Fig. 50), the voltage dip is much more severe than when using the TOWI method (Fig. 48). The SCV technique operates a little faster than the dual-quadrilateral technique because there is no qualifying OST timer in the SCV-assisted OST logic.

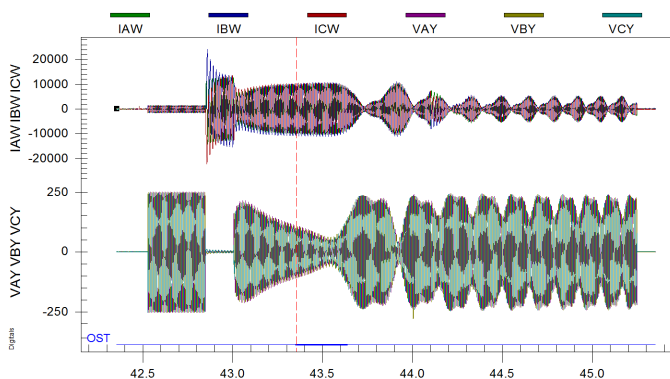


Fig. 47. TOWI using the dual-quadrilateral technique.

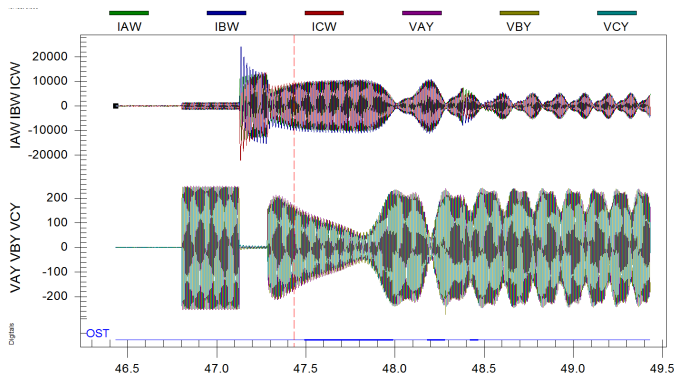


Fig. 48. TOWI using the SCV technique.

Fig. 49 and Fig. 50 show the TOWO method for both the dual-quadrilateral and the SCV techniques. The OST bit asserted and tripped the relay during the first slip cycle, as expected with TOWO. It is necessary to perform extensive system studies to determine if the power system can withstand depressed voltage long enough for the power swing to be detected and tripped. Consideration of the voltage levels at the slowest swing rate will help to determine if TOWI is appropriate.

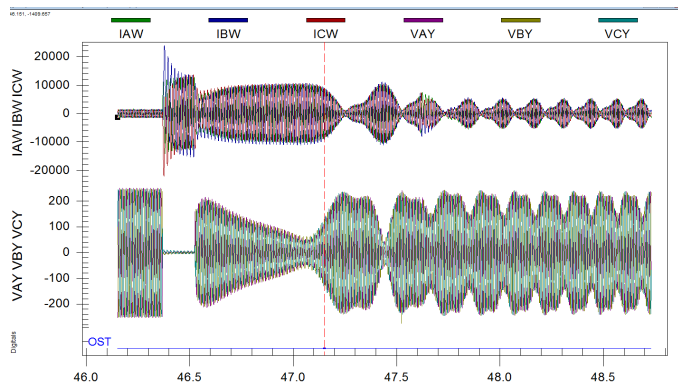


Fig. 49. TOWO using the dual-quadrilateral technique.

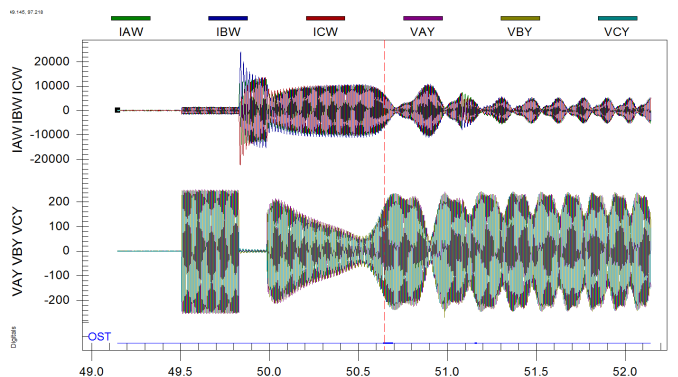


Fig. 50. TOWO using the SCV technique.

VII. TEST OF PSB AND OST SCHEMES

One of the challenges after a PSB or tripping scheme has been set is how to validate that the scheme operates correctly during an actual OOS or power swing condition on the power system. The solution to this challenge is relatively simple: test the system using data obtained during a true power system OOS or power swing condition. Alternatively, if the power system is modeled in an electromagnetic transients program, create different power swing scenarios, such as stable and unstable swings, and ensure that the relay operates as set.

Testing power swing protection functions with relay test equipment that cannot reproduce the type of signals present during power swings is difficult, if not impossible. The practice of using older relay test sets and ramping the currents, voltages, and/or frequency is not a preferred or recommended approach.

Modern relay test equipment can replay COMTRADE signals captured during actual power swings by relays or digital fault recorders or generated by an electromagnetic transients program. The most appropriate test method to verify relay performance during a stable or unstable power swing is to generate COMTRADE cases from transient simulations and test the relay using modern test equipment. Using this methodology, we can verify if the relay will perform satisfactorily during OOS conditions. Users should decide whether to use generic COMTRADE test cases or to model the dynamics of the actual power system where they plan to apply the power swing protection relays. Note that generic OOS test cases do not reflect true conditions for a particular application.

In this paper, we discuss two methods of power swing detection. One method requires detailed knowledge of the power system behavior during an OOS or power swing condition, such as the swing rate of the system and its impedance trajectory. The other method requires no knowledge of the behavior of the system, and as such, no power swing studies are required. If the first method is used to set the PSB and/or tripping logic, then it is quite reasonable to assume that COMTRADE-type files of different simulated OOS or power swing conditions from the modeled power system can be provided to test personnel for the testing of the OOS scheme. If, on the other hand, the second method (settingless) is used for detection of a power swing condition, then these types of files are not readily available to test personnel. It will defeat the objective of the second method if test personnel need to create these files in order to test the scheme. The question of how to test an OOS or power swing scheme when no stored testing files are available is discussed further in this section.

Power swings or OOS conditions can be generated by simply creating a mathematical model of a two-source equivalent power system (as shown in Fig. 51). The following is a discussion of how test personnel can use simple mathematical tools at their disposal to generate a test case to verify the correct operation of PSB or OST schemes. In a mathematical software package, we simply write the equations for the voltages at the two sources, an example of which is shown in (22).

$$\begin{aligned} VA_S(t) &= \sqrt{2} \cdot 67 \sin(2\pi f_S \cdot t + \theta_S) \\ VA_R(t) &= \sqrt{2} \cdot 65 \sin(2\pi f_R \cdot t + \theta_R) \end{aligned} \quad (22)$$

By decreasing the frequency of one of the two sources over time to a desired swing rate, an OOS or power swing condition is created. By calculating the voltage difference between the two sources and using the total system impedance, the system current can be calculated. The typical swing rate of a power swing condition on most power systems is between 4 and 7 Hz [6].

Fig. 51 is a diagram of a simple two-source equivalent power system that can be used to generate voltages and currents representative of a power swing condition.

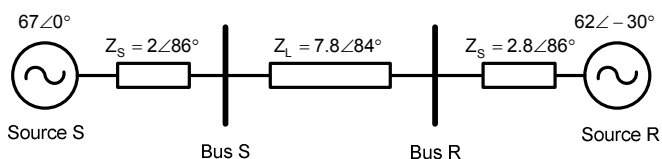


Fig. 51. A two-source equivalent system used to generate the voltages and currents in a mathematical model.

The currents and voltages shown in Fig. 52 represent the currents and voltages as observed at Bus S of the equivalent two-source power system shown in Fig. 51. In this simulation, the frequency of Source R decreases exponentially until the system has a final slip rate of 1 Hz. The currents and voltages

are then output in a COMTRADE format. In this format, the event can be played back into a power swing protection scheme.

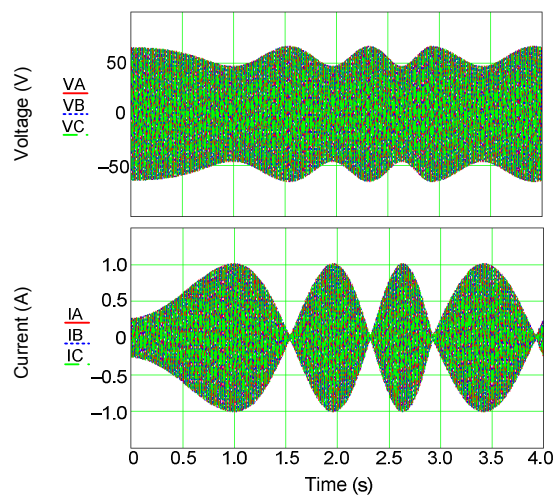


Fig. 52. Plot of the voltages and currents for a simulated power swing condition.

Fig. 53 is a plot of the positive-sequence impedance Z_1 as calculated by a power swing protection scheme located at Bus S. Viewing the power swing condition in the impedance plane allows us to adapt the power swing condition to any condition that we want to test and also enables us to correlate it with the distance protection scheme.

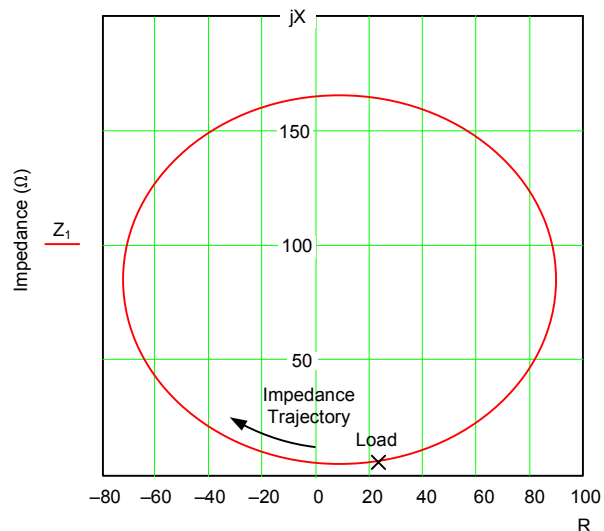


Fig. 53. The impedance trajectory of the positive-sequence impedance generated using the voltages and currents in Fig. 52.

The COMTRADE test files generated by the method discussed so far can be used to test the PSB scheme and the OST schemes, where tripping is only initiated after the positive-sequence impedance has traversed the positive-sequence impedance plane more than a certain number of times (a traversing of the positive-sequence impedance plane is synonymous with a pole slip of a machine). To visualize how many times the positive-sequence impedance has

traversed the positive-sequence impedance plane, it is useful to also decrease the voltage of one of the sources at the same time as decreasing its frequency; the decrease in voltage results in the impedance loop becoming smaller, as shown in Fig. 54.

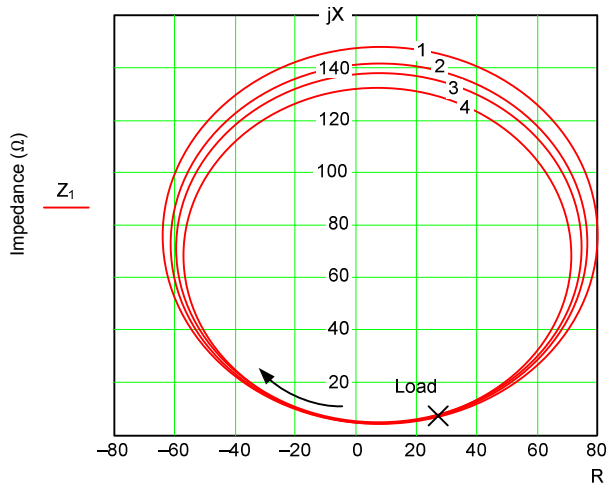


Fig. 54. The impedance trajectory of the positive-sequence impedance when both the voltage and frequency are decreased exponentially (1 represents the first trajectory loop, 2 the second trajectory loop, and so on).

One additional important test case is to verify that an OST scheme remains stable and does not initiate a trip if the system experiences a stable power swing. To simulate this condition, both the voltage and frequency at one source are ramped down and back up again. This results in the positive-sequence impedance traversing the impedance plane initially in one direction and then turning around and returning to the same segment in the impedance plane, as shown in Fig. 55.

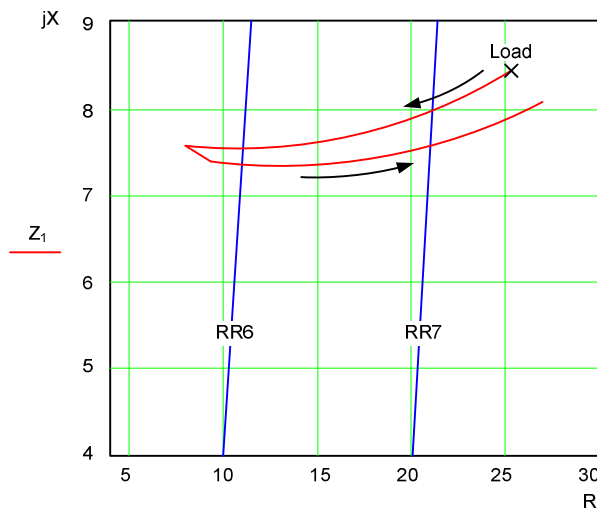


Fig. 55. Positive-impedance trajectory for a stable power swing condition; the impedance enters the blinders (RR6 and RR7) from the right-hand side and exits on the right-hand side.

The mathematical test cases described and discussed here can be used not only to test schemes where the settlingless OOS protection scheme is implemented but also to test a scheme set using the traditional OOS protection or blocking

scheme. Should test personnel not be able to create these test cases, they should contact a relay manufacturer to assist them in generating the test cases.

VIII. CONCLUSION

This paper illustrates many different power swing detection methods and provides examples of two specific methods that can be used to successfully detect a power swing condition in a power system following a disturbance. OST is also discussed, including when it should be used and how it should be set up based on system characteristics.

The first of the two example methods, the dual-quadrilateral method, requires an extensive study of the power system with faults applied during different operating conditions. The user has to analyze the trajectory of the Z_1 impedance in addition to the rate at which the Z_1 impedance traverses the Z_1 impedance plane. Using these data, the parameters for the inner and outer quadrilateral elements are established. The rate (speed) at which the Z_1 impedance traverses the Z_1 plane is used in determining the parameters of the PSB timer. This timer has to accommodate the fastest stable swing that the system may be subjected to, if OST for unstable swings is required. It is not always possible to set the quadrilateral elements and timers to coordinate properly, especially if the protected line is long and heavily loaded. For these cases, special measures have to be taken to ensure the correct detection of a swing condition.

The second method is based on the SCV and is not dependent on any system source or line impedances (as shown in Section IV). Therefore, this method does not require any system studies to be conducted and, as such, does not require any user-defined settings.

This paper shows that both the dual-quadrilateral and the SCV methods can successfully be used to detect a power swing in a power system. Using field cases, this paper also illustrates that to successfully detect an OOS condition using the dual-quadrilateral method, we must correctly set the quadrilateral element parameters, whereas the SCV method does not require us to apply settings to the relay.

This paper also discusses theories and applications of OST. OST is necessary for unstable power swings to make sure that a power system can be safely separated before an OOS condition causes further damage to the system or increases the area of an outage. Depending on system behavior and characteristics, two OST methods can be implemented: TOWI and TOWO. TOWI protects the power system from prolonged times of depressed voltage or elevated current that could damage equipment in the power system.

In conclusion, there are many different power swing detection methods that can be used to protect a power system from OOS conditions, each of which has its own benefits and drawbacks. Two specific methods are presented in this paper for PSB and OST. The SCV method allows the user to successfully apply PSB detection without any knowledge of the dynamic response of the power system.

IX. REFERENCES

- [1] C. R. Mason, *The Art and Science of Protective Relaying*. John Wiley & Sons, Inc., New York, 1956.
- [2] N. Fischer, G. Benmouyal, and S. Samineni, "Tutorial on the Impact of the Synchronous Generator Model on Protection Studies," proceedings of the 35th Annual Western Protective Relay Conference, Spokane, WA, October 2008.
- [3] G. Benmouyal, D. Hou, and D. Tziouvaras, "Zero-Setting Power-Swing Blocking Protection," proceedings of the 31st Annual Western Protective Relay Conference, Spokane, WA, October 2004.
- [4] D. Hou, S. Chen, and S. Turner, "SEL-321-5 Relay Out-of-Step Logic," SEL Application Guide (AG97-13), 2009. Available: <http://www.selinc.com>.
- [5] IEEE Power System Relaying Committee WG D6, "Power Swing and Out-of-Step Considerations on Transmission Lines," July 2005. Available: <http://www.pes-psrc.org>.
- [6] J. Mooney and N. Fischer, "Application Guidelines for Power Swing Detection on Transmission Systems," proceedings of the 32nd Annual Western Protective Relay Conference, Spokane, WA, October 2005.
- [7] J. Holbach, "New Blocking Algorithm for Detecting Fast Power Swing Frequencies," proceedings of the 30th Annual Western Protective Relay Conference, Spokane, WA, October 2003.
- [8] Q. Verzosa, "Realistic Testing of Power Swing Blocking and Out-of-Step Tripping Functions," proceedings of the 38th Annual Western Protective Relay Conference, Spokane, WA, October 2011.
- [9] G. Benmouyal, E. O. Schweitzer, III, and Armando Guzmán, "Synchronized Phasor Measurement in Protective Relays for Protection, Control, and Analysis of Electric Power Systems," proceedings of the 29th Annual Western Protective Relay Conference, Spokane, WA, October 2002.
- [10] Y. Ohura, M. Suzuki, K. Yanagihashi, M. Yamaura, K. Omata, and T. Nakamura, S. Mitamura, and H. Watanabe, "A Predictive Out-of-Step Protection System Based on Observation of the Phase Difference Between Substations," *IEEE Transactions on Power Delivery*, Vol. 5, No. 4, October 1990.
- [11] A. Guzmán, V. Mynam, and G. Zweigle, "Backup Transmission Line Protection for Ground Faults and Power Swing Detection Using Synchrophasors," proceedings of the 34th Annual Western Protective Relay Conference, Spokane, WA, October 2007.
- [12] C. W. Taylor, J. M. Haner, L. A. Hill, W. A. Mittelstadt, and R. L. Cresap, "A New Out-of-Step Relay With Rate of Change of Apparent Resistance Augmentation," *IEEE Transactions on Power Apparatus and Systems*, Vol. PAS-102, No. 3, March 1983.
- [13] J. M. Haner, T. D. Laughlin, and C. W. Taylor, "Experience with the R-Rdot Out-of-Step Relay," *IEEE Transactions on Power Delivery*, Vol. 1, No. 2, April 1986.
- [14] F. Ilar, "Innovations in the Detection of Power Swings in Electrical Networks," Brown Boveri Publication CH-ES 35-30.10E, 1997.
- [15] D. A. Tziouvaras and D. Hou, "Out-of-Step Protection Fundamentals and Advancements," proceedings of the 30th Annual Western Protective Relay Conference, Spokane, WA, October 2003.
- [16] W. A. Elmore, "Out-of-Step Relaying System Selection," Silent Sentinels, RPL 76-3, Westinghouse Electric Corporation, September 1976.

X. BIOGRAPHIES

Normann Fischer received a Higher Diploma in Technology, with honors, from Witwatersrand Technikon, Johannesburg, in 1988, a BSEE, with honors, from the University of Cape Town in 1993, and an MSEE from the University of Idaho in 2005. He joined Eskom as a protection technician in 1984 and was a senior design engineer in the Eskom protection design department for three years. He then joined IST Energy as a senior design engineer in 1996. In 1999, he joined Schweitzer Engineering Laboratories, Inc. as a power engineer in the research and development division. Normann was a registered professional engineer in South Africa and a member of the South Africa Institute of Electrical Engineers. He is currently a member of IEEE and ASEE.

Gabriel Benmouyal, P.E., received his BAsC in electrical engineering and his MASc in control engineering from Ecole Polytechnique, Université de Montréal, Canada. He then joined Hydro-Québec as an instrumentation and control specialist. He worked on different projects in the fields of substation control systems and dispatching centers. In 1978, he joined IREQ, where his main fields of activity were the application of microprocessors and digital techniques for substations and generating station control and protection systems. In 1997, he joined Schweitzer Engineering Laboratories, Inc. as a principal research engineer. Gabriel is a registered professional engineer in the Province of Québec and an IEEE senior member and has served on the Power System Relaying Committee since May 1989. He holds more than six patents and is the author or coauthor of several papers in the fields of signal processing and power network protection and control.

Daqing Hou received BSEE and MSEE degrees at the Northeast University, China, in 1981 and 1984, respectively. He received his PhD in Electrical and Computer Engineering at Washington State University in 1991. Since 1990, he has been with Schweitzer Engineering Laboratories, Inc., where he has held numerous positions, including development engineer, application engineer, research and development manager, and principal research engineer. He is currently the research and development technical director for East Asia. His work includes power system modeling, simulation, signal processing, and advanced protection algorithm design. His research interests include multivariable linear systems, system identification, and signal processing. Daqing holds multiple patents and has authored or coauthored many technical papers. He is a senior member of IEEE.

Demetrios Tziouvaras received a BSEE and MSEE from the University of New Mexico and Santa Clara University, respectively. He is an IEEE senior member and a member of the Power Engineering Society, the Power System Relaying Committee, and CIGRE. He joined Schweitzer Engineering Laboratories, Inc. in 1998 and currently holds the position of senior research engineer. From 1980 until 1998, he was with Pacific Gas and Electric, where he held various protection engineering positions, including principal protection engineer responsible for protection design standards, new technologies, and substation automation. He holds multiple patents and is the author or coauthor of many IEEE and protective relay conference papers. His work includes power system modeling, simulation, and design of advanced protection algorithms.

John Byrne-Finley received a BSEE and an MSEE with a power emphasis from the University of Idaho in 2007 and 2009, respectively. He joined Schweitzer Engineering Laboratories, Inc. in 2009 and is now a power engineer in the research and development division. John is a coauthor of several papers on electric vehicles and battery systems and is an active IEEE member.

Brian Smyth received a BS in general engineering with an electrical option and an MSEE from Montana Tech of the University of Montana in 2006 and 2008, respectively. He joined Montana Tech as a visiting professor in 2008 and taught classes in electrical circuits, electric machinery, instrumentation and controls, and power systems. He joined Schweitzer Engineering Laboratories, Inc. in 2009 as an associate power engineer in the research and development division. Brian is a coauthor of several papers on battery impedance measurement and is an active IEEE member.